Supporting Information for

Oblique convergence causes both thrust and strike-slip ruptures during the 2021 M 7.2 Haiti earthquake

Ryo Okuwaki[1,2,3] & **Wenyuan Fan**[4]

[1]Mountain Science Center, University of Tsukuba, Tsukuba, Ibaraki 305-8572, Japan

[2]Faculty of Life and Environmental Sciences, University of Tsukuba, Tsukuba, Ibaraki 305-8572, Japan

[3]COMET, School of Earth and Environment, University of Leeds, Leeds LS2 9JT, UK

[4]Scripps Institution of Oceanography, UC San Diego, La Jolla, California 92093, USA

Contents

Corresponding author: Ryo Okuwaki, `rokuwaki@geol.tsukuba.ac.jp`

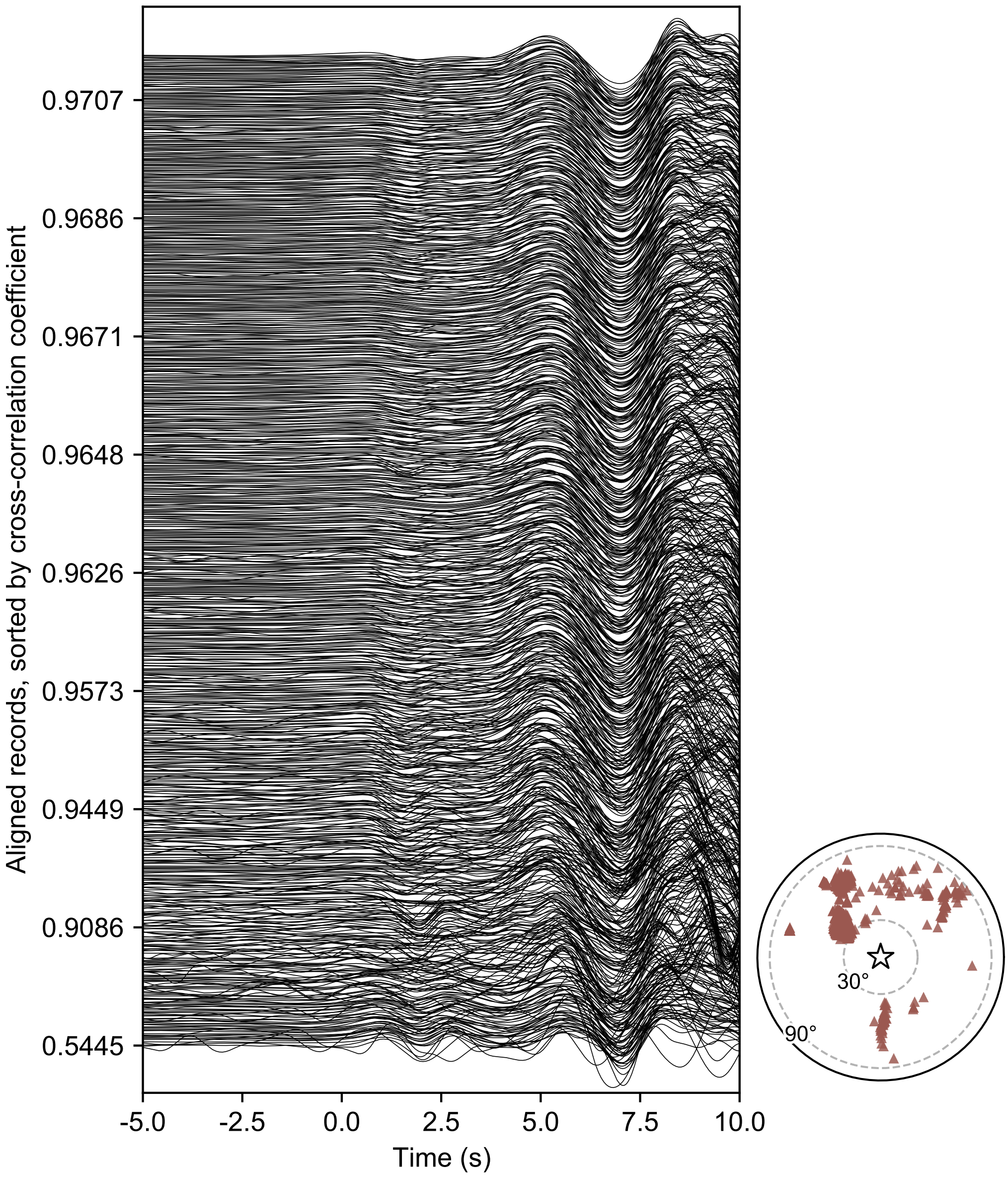

Figure S1. Self-normalized traces used for the back-projection analysis. The records are band-pass filtered at 0.2–1 Hz. The right panel shows the station distribution.

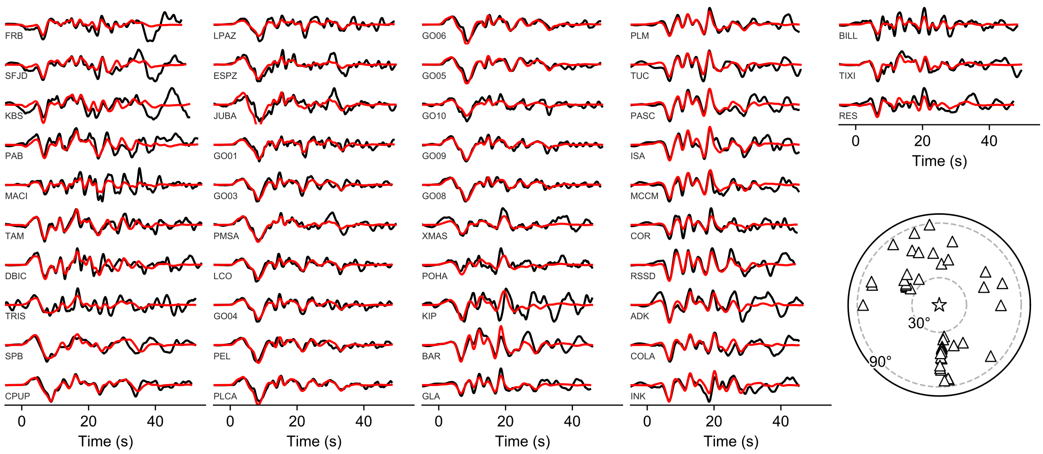

Figure S2. The observed (black) and synthetic (red) waveforms of the optimal finite-fault model. The station code is shown in each panel. The lower-right panel shows the station distribution.

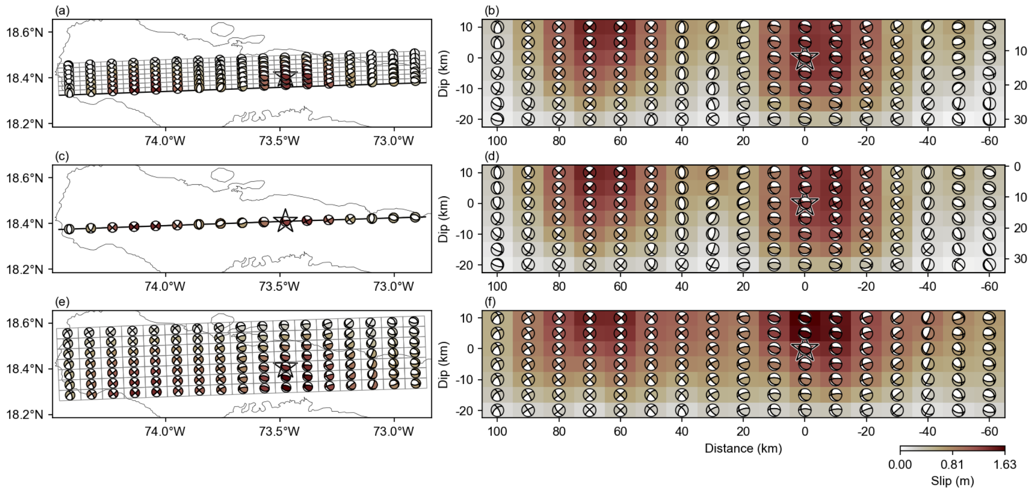

Figure S3. Finite-fault models of three different model-domain geometries using dipping planes of (a,b) 64°, (c,d) 90°, and (e,f) 0°. The horizontal model domain (e,f) is placed at 10-km depth.

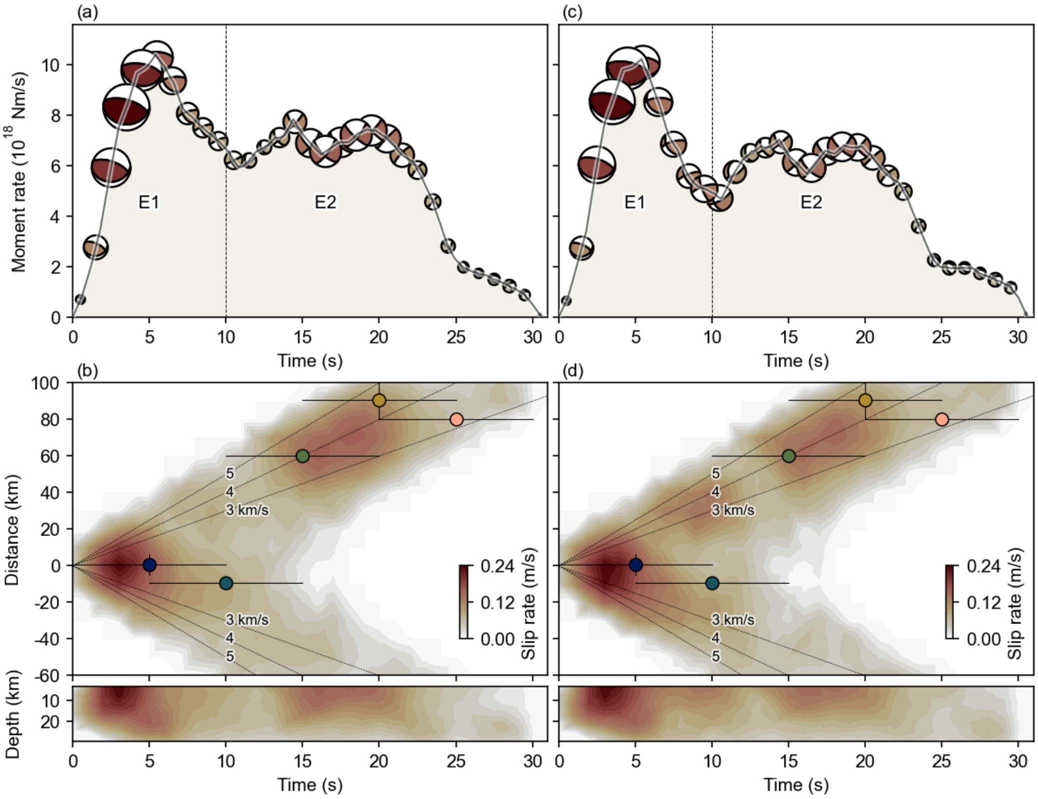

Figure S4. Resolvability test for the finite-fault inversion. (a,b) show the input model (Fig. 3) and (c,d) show the output model. (a,c) The moment rate functions of the finite-fault models. The beach balls are the centroid moment tensor solutions of the finite-fault models for the snapshot time windows of every 1 s. (b,d) The spatiotemporal distributions of the finite-faults model in comparison with the back-projection results. The distributions are projected along a direction of 268° azimuth (middle panel) and along the depth of the finite-fault model domain (bottom panel). The contours show the slip rate distributions. The colored dots are from the back-projection results. The vertical bars show the uncertainty estimates from the jackknife re-sampling exercise and the horizontal bars show the stacking window lengths. The black lines are the reference rupture speeds.

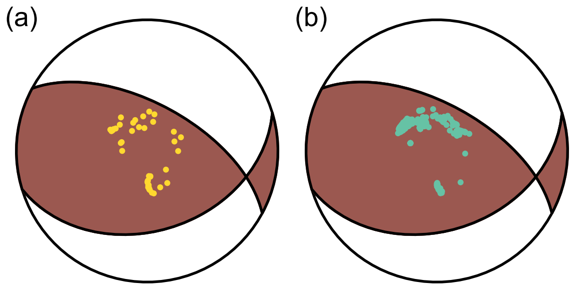

Figure S5. Station distributions used for (a) finite-fault and (b) back-projection analyses. The station locations are projected as yellow (finite-fault model) and green (back-projection) dots at the *P* wave ray piercing points at the lower focal sphere. The beach ball is the double-couple solution of the centroid moment tensor shown in Fig. 2b at 0–1 s.

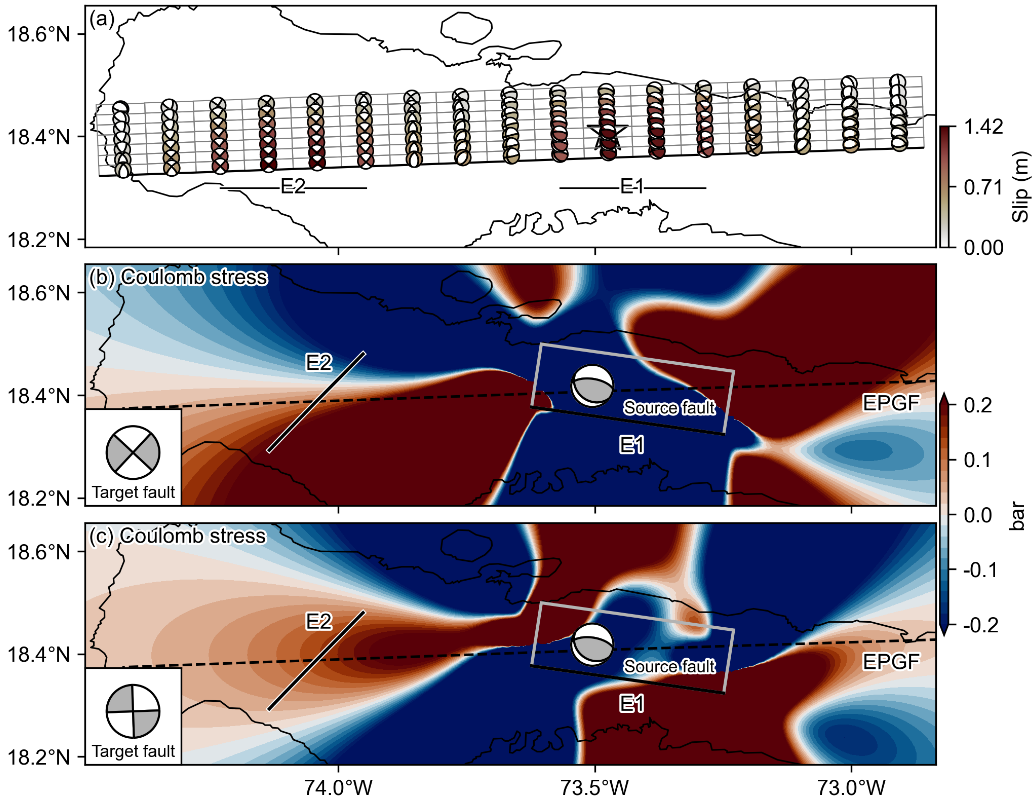

Figure S6. Coulomb stress analyses of the 2021 Haiti earthquake. (a) The optimal finite-fault solution of the 2021 Haiti earthquake as shown in Fig. 1. Lower panels show the Coulomb stress changes at 10-km depth for a target fault geometry of (b) 223°/90°/0° (strike/dip/rake) and the EPGF geometry of (c) 268°/90°/0°. The Coulomb stresses are calculated with a friction coefficient of 0.4, poison ratio of 0.25, and Young's modulus of $8{\times}10^5$ bars. The source fault geometry is set as 278.4°/62.7°/77.1° with an extent of 40-km in length and 30-km in width. The shallow edge of the source fault is at 0.8-km depth. We assume a uniform slip of 1.37 m for the source fault based on our rupture episode E1 (Fig. 1). The E2 location is outlined by a solid black line.

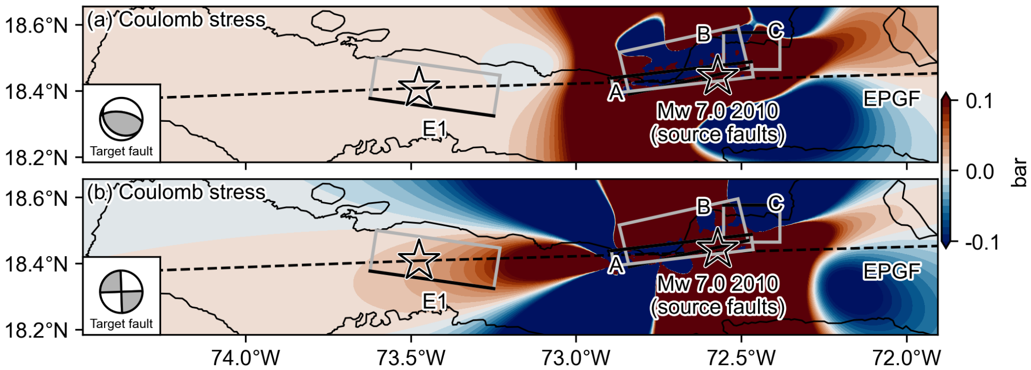

Figure S7. Coulomb stress analyses of the 2010 Haiti earthquake. Coulomb stress changes at 12-km depth on a target fault (a) of 278.4°/62.7°/77.1° (strike/dip/rake) as E1 and the EPGF geometry (b) of 268°/90°/0° . The Coulomb stresses are calculated with a friction coefficient of 0.4, poison ratio of 0.25, and Young's modulus of $8{\times}10^5$ bars. The source fault geometries of the 2010 Haiti earthquake are from Hayes et al. (2010). The finite-fault model of the 2010 Haiti earthquake is from Hayes et al. (2010) archived at SRCMOD (Mai & Thingbaijam, 2014) (http://equake-rc.info/SRCMOD/searchmodels/viewmodel/s2010HAITIx01HAYE/). For the 2010 Haiti earthquake, we assume a pure vertical slip for fault B and left-lateral slip for faults A and C based on the model of Hayes et al. (2010).

References in the Supporting Information

Hayes, G. P., Briggs, R. W., Sladen, A., Fielding, E. J., Prentice, C., Hudnut, K., ... Simons, M. (2010). Complex rupture during the 12 January 2010 Haiti earthquake. *Nat. Geosci.*, *3*(11), 800–805. doi:10.1038/ngeo977

Mai, P. M., & Thingbaijam, K. K. (2014). SRCMOD: An online database of finite-fault rupture models. *Seismol. Res. Lett.*, *85*(6), 1348–1357. doi:10.1785/0220140077